ARTICLE

Pharmacokinetics of Capecitabine and Four Metabolites in a Heterogeneous Population of Cancer Patients: A Comprehensive Analysis

Bart A.W. Jacobs[1,2,*], Maarten J. Deenen[3,4], Markus Joerger[1,2], Hilde Rosing[2], Niels de Vries[2], Didier Meulendijks[1,5], Annemieke Cats[6], Jos H. Beijnen[2,7], Jan H.M. Schellens[1,7] and Alwin D.R. Huitema[2,8]

Capecitabine is an oral prodrug of the anticancer drug 5-fluorouracil (5-FU). The primary aim of this study was to develop a pharmacokinetic model for capecitabine and its metabolites, 5′-deoxy-5-fluorocytidine (dFCR), 5′-deoxy-5-fluorouridine (dFUR), 5-FU, and fluoro-β-alanine (FBAL) using data from a heterogeneous population of cancer patients ($n = 237$) who participated in seven clinical studies. A four-transit model adequately described capecitabine absorption. Capecitabine, dFCR, and FBAL pharmacokinetics were well described by two-compartment models, and dFUR and 5-FU were subject to flip-flop pharmacokinetics. Partial and total gastrectomy were associated with a significantly faster capecitabine absorption resulting in higher capecitabine and metabolite peak concentrations. Patients who were heterozygous polymorphic for a genetic mutation encoding dihydropyrimidine dehydrogenase, the *DPYD**2A mutation, demonstrated a 21.5% (relative standard error 11.2%) reduction in 5-FU elimination. This comprehensive population model gives an extensive overview of capecitabine and metabolite pharmacokinetics in a large and heterogeneous population of cancer patients.

Study Highlights

WHAT IS THE CURRENT KNOWLEDGE ON THIS TOPIC?
☑ The oral anticancer drug capecitabine is the most frequently used oral cytotoxic agent. After intake, capecitabine is rapidly absorbed and extensively metabolized.

WHAT QUESTION DID THIS STUDY ADDRESS?
☑ The aim was to assess the pharmacokinetics of capecitabine and its metabolites for a large and hetero-geneous population of cancer, including patients who underwent (partial) gastrectomy and patients polymor-phic for *DPYD*.

WHAT DOES THIS STUDY ADD TO OUR KNOWLEDGE?
☑ Capecitabine and metabolite pharmacokinetics are highly variable across cancer patients. Absorption of capecitabine is more rapid after (partial) gastrectomy. Exposure to the metabolite 5-fluorouracil is increased by 21.5% for *DPYD**2A mutation carriers.

HOW MIGHT THIS CHANGE DRUG DISCOVERY, DEVELOPMENT, AND/OR THERAPEUTICS?
☑ There is no need for dose adaptation after (partial) gas-trectomy. The effect of the *DPYD**2A mutation is less than would be expected, suggesting a lower dose reduction for this patient population than currently recommended.

Capecitabine is an oral prodrug of 5-fluorouracil (5-FU) and is frequently used for the treatment of breast, colorectal, and gastric cancer. After oral administration, capecitabine is rapidly and completely absorbed. Thereafter, it is metab-olized to subsequently 5′-deoxy-5-fluorocytidine (dFCR), 5′-deoxy-5-fluorouridine (dFUR), and 5-FU via a three-step enzymatic cascade involving the enzymes carboxylesterase, cytidine deaminase (CDA), and thymidine phosphorylase, respectively (**Figure S1**).[1,2] Approximately 80% of 5-FU is rapidly catabolized to inactive metabolites, and a small proportion of 5-FU is intracellularly anabolized to cytotoxic metabolites.[3,4] The enzyme dihydropyrimidine dehydro-genase (DPD) catalyzes the initial step of 5-FU catabolism that leads to the formation of 5,6-dihydro-5-fluorouracil.[5] 5,6-dihydro-5-fluorouracil is eventually metabolized to fluo-ro-β-alanine (FBAL), which is cleared renally.[2]

Several studies have been conducted to investigate the pharmacokinetics (PK) of capecitabine and its me-tabolites.[2] Most capecitabine PK studies have employed noncompartmental PK analysis, which does not allow for

[1]Department of Clinical Pharmacology, The Netherlands Cancer Institute, Amsterdam, The Netherlands; [2]Department of Pharmacy & Pharmacology, The Netherlands Cancer Institute, Amsterdam, The Netherlands; [3]Department of Clinical Pharmacy, Catharina Hospital, Eindhoven, The Netherlands; [4]Department of Clinical Pharmacology and Toxicology, Leiden University Medical Centre, Leiden, The Netherlands; [5]Dutch Medicines Evaluation Board, Utrecht, The Netherlands; [6]Department of Gastrointestinal Oncology, The Netherlands Cancer Institute, Amsterdam, The Netherlands; [7]Division of Pharmaco-epidemiology & Clinical Pharmacology, Science Faculty, Utrecht Institute for Pharmaceutical Sciences, Utrecht University, Utrecht, The Netherlands; [8]Department of Clinical Pharmacy, University Medical Center Utrecht, Utrecht, The Netherlands. *Correspondence: Bart A.W. Jacobs (b.jacobs@nki.nl)
Received: April 18, 2019; accepted: September 6, 2019. doi:10.1002/psp4.12474

the simultaneous analysis of parent and metabolite PK.[2] Moreover, this approach does not allow for the appropriate quantification of between-subject and between-occasion variabilities in parent and metabolite PK parameters.

A few population PK studies of capecitabine have been performed. Two previously developed population PK models incorporated only PK data of the metabolites dFUR, 5-FU, and FBAL.[6,7] Another study only described a relatively small population and did not include the final metabolite FBAL.[8]

We have collected PK data of capecitabine and metabolites in several studies of various patient populations and treatment regimens. One of the studies exclusively included patients carrying the *DPYD**2A allele: an allele encoding nonfunctional DPD enzyme that is strongly associated with severe fluoropyrimidine-induced toxicity.[9–13] In addition, the current study includes patients who previously underwent a partial or total gastrectomy for the treatment of gastric cancer. Little is known about the PK of capecitabine and the metabolites in these specific subpopulations. The aim of this study was to develop a comprehensive population PK model by the integration of all available PK data.

RESULTS

Pharmacokinetic data of 237 patients were included for the population PK analysis. This resulted in the availability of a total of 8,988 observations for capecitabine, dFCR, dFUR, 5-FU, and FBAL. The patients received a median (range)

capecitabine dose of 1,650 (300–2,600) mg. For 63 of 237 patients, the PK data of two occasions were available. For one patient participating in study 1 (see **Table 1**), the PK data were collected on three occasions. For all other patients, the PK data were available from a single occasion. The number of patients and the capecitabine dose per study are summarized in **Table 1**. Patient characteristics are shown in **Table 2**.

The PK database included 560 observations below the lower limit of quantification (LLoQ) that were imputed as LLoQ/2. The percentage of observations below the LLOQ for capecitabine, dFCR, dFUR, 5-FU, and FBAL were 5.0%, 4.7%, 4.8%, 10.1%, and 7.4%, respectively. A graphical overview of the PK data is shown in **Figure S2**. Capecitabine demonstrated rapid absorption and elimination. The average capecitabine peak concentration was observed approximately 0.5 hours after dosing. For dFCR, dFUR, and 5-FU, the average peak level was found around 1 hour after dosing. The peak concentration of FBAL appeared relatively late: approximately 2.5 hours after dose administration. The plasma concentration-time profiles of dFCR, dFUR, and 5-FU demonstrated similar patterns. FBAL was less rapidly eliminated from plasma than the other compounds.

Population PK model
The structure of the final model is depicted in **Figure 1**, and the final parameter estimates are summarized in **Table 3**. A detailed description of model development is provided in the following two paragraphs.

Table 1 Summary of the clinical studies

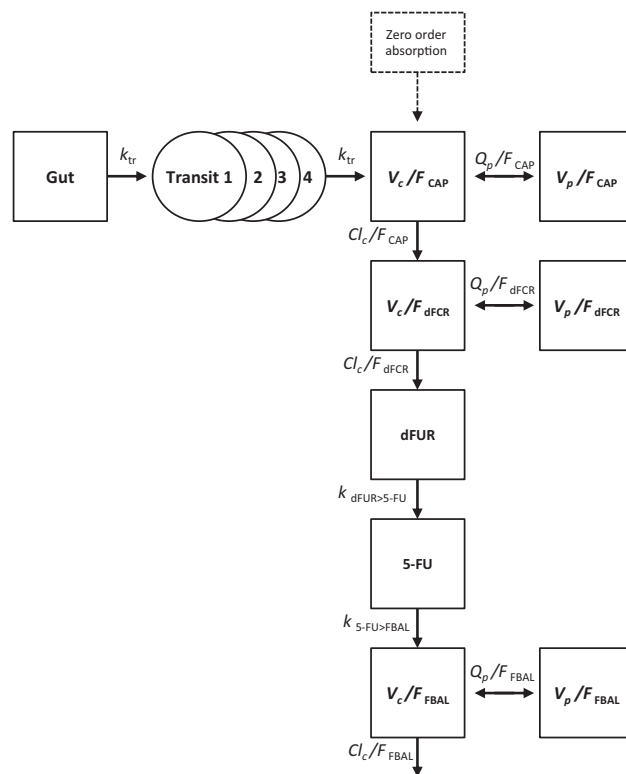| Study number	Number of subjects	Median (range) capecitabine dose (mg)	Study description	Cotreatment	Sampling design	Sampling schedule (h after intake)	References
1	19	800 (300–1,000)	Study of cancer patients carrying the *DPYD**2A risk allele who received ~ 50% of the registered capecitabine dose	Variable	Rich sampling treatment day 1	0.25, 0.5, 1, 2, 3, 4, 5, 6, 8	[9]
2	30	1,650 (1,150–1,700)	Phase I study in patients with cancer of the stomach or gastroesophageal junction	Docetaxel and oxaliplatin	Rich sampling treatment day 1	0, 0.5, 1, 2, 3, 4, 6, 8	[21]
3	31	1,500 (1,000–2,000)	Phase I–II study in patients with gastric and esophageal cancer; capecitabine treatment was started after tumor resection	Radiotherapy	Rich sampling on days 22 and 43 of treatment	0, 0.25, 0.5, 0.75, 1, 1.5, 2, 3, 4	[22]
4	41	1,150 (300–1,500)	Phase I–II study in patients with gastric and esophageal cancer; capecitabine treatment was started after tumor resection	Radiotherapy and cisplatin	Rich sampling on days 22 and 43 of treatment	0, 0.25, 0.5, 0.75, 1, 1.5, 2, 3, 4	[23,24]
5	48	1,925 (1,000–2,600)	Study to determine proteomic profile and capecitabine pharmacokinetics in patients with advanced colorectal cancer	Oxaliplatin	Rich sampling treatment day 1	0, 0.5, 1, 1.5, 2, 3, 4, 5, 6	[25]
6	50	2,000 (1,300–2,000)	Study to determine proteomic profile and pharmacokinetics in patients with advanced gastric cancer	Cisplatin and epirubicin	Rich sampling treatment day 1	0, 0.5, 1, 1.5, 2, 3, 4, 5, 6, 8	[25]
7	18	1,475 (900–1,650)	Phase I study in patients with advanced anal cancer	Radiotherapy and mitomycin-c	Rich sampling treatment day 1	0, 0.25, 0.5, 1, 2, 3, 4, 6, 8	[26]

DPYD, dihydropyrimidine dehydrogenase.

Table 2 Characteristics of the study population and potential covariates study population

Characteristic	Unit	Value
Total number of subjects	n	237
Gender		
Male	n (%)	159 (67.1)
Female	n (%)	78 (32.9)
Age, mean (range)	Years	57.5 (27.8–77.8)
Gastric surgery		
No gastrectomy	n (%)	154 (65.0)
Total gastrectomy	n (%)	24 (10.1)
Partial gastrectomy	n (%)	44 (18.6)
Esophagogastrectomy	n (%)	15 (6.3)
DPYD*2A		
Wild type	n (%)	216 (91.1)
Heterozygous mutant	n (%)	21 (8.9)
DPYD c.2846A>T		
Wild type	n (%)	207 (87.3)
Heterozygous mutant	n (%)	11 (4.6)
Unknown	n (%)	19 (8.0)
DPYD c.1236G>A		
Wild type	n (%)	159 (67.1)
Heterozygous mutant	n (%)	11 (4.6)
Unknown	n (%)	67 (28.3)
CDA c.79A>C		
Wild type	n (%)	79 (33.3)
Heterozygous mutant	n (%)	62 (26.2)
Homozygous mutant	n (%)	22 (9.3)
Unknown	n (%)	74 (31.2)

DPYD, dihydropyrimidine dehydrogenase; *CDA*, cytidine deaminase.

Figure 1 Representation of the population pharmacokinetic model of capecitabine, dFCR, dFUR, 5-FU, and FBAL. CAP, capecitabine; CL$_c$/F, apparent clearance of central compartment; dFCR, 5′-deoxy-5-fluorocytidine; dFUR, 5′-deoxy-5-fluorouridine; 5-FU, 5-fluorouracil; FBAL, fluoro-β-alanine; k_{tr}, transit rate constant; Q_p/F, apparent intercompartmental clearance; V_c/F, apparent central volume of distribution; V_p/F, apparent peripheral volume of distribution.

Capecitabine PK

The capecitabine absorption rate was highly variable between subjects and occasions. In 95 of the 301 occasions (31.6%), capecitabine peak concentrations were observed at the first observation after drug administration. For these curves, adequate estimation of the absorption phase was not possible. With the different absorption models tested, these curves caused run failure and/or estimation problems. Therefore, a zero-order absorption process in which the dose was fully absorbed between time of capecitabine intake and the time of the first observation was assumed for these individual curves. Interestingly, this was necessary in 21 of the 42 occasions from the patients who underwent total gastrectomy. For the remaining 206 occasions (68.4%), a first-order transit absorption model including four transit compartments most accurately described the absorption process but resulted in a slight underprediction of maximum plasma concentrations (C$_{max}$) of capecitabine and metabolites. Increasing the number of transit compartments did not result in a significant improvement of the model fit. Visual inspection of the random-effect distribution on the transit rate constant (k_{tr}) suggested that capecitabine absorption occurred relatively fast for the patients who previously underwent gastrectomy for advanced gastric cancer. Therefore, partial gastrectomy and total gastrectomy were included as categorical covariates

on the transit rate constant, which resulted in a significantly improved model fit (**Table S1**).

The mean transit time, which was calculated by (the number of transit compartments + 1)/ k_{tr}, was 0.67 and 0.31 hours for patient who underwent partial and total gastrectomy, respectively. For the other patients, the estimated mean transit time was 0.98 hours. Between-subject variability (BSV) and between-occasion variability (BOV) on the k_{tr} were successfully estimated and were found to be relatively large.

Capecitabine distribution and elimination was best described by a two-compartmental model with linear intercompartmental clearance. BSV terms for the apparent central clearance (CL$_c$/F$_{CAP}$) and volume of distribution (V_c/F$_{CAP}$) were included. In particular, BSV on V_c/F$_{CAP}$ was estimated to be large (132.1%). There was a significant correlation between BSV on CL$_c$/F$_{CAP}$ and BSV on V_c/F$_{CAP}$.

Metabolite population PK modeling

The population PK model of capecitabine was extended with the four metabolites. As shown in **Figure S2**, the mean plasma concentration-time curve for the first metabolite, dFCR, followed a biexponential decay. A two-compartmental model with linear clearance, which included a BSV term on

Table 3 Parameter estimates of the population pharmacokinetic model of capecitabine, dFCR, dFUR, 5-FU and FBAL

Parameter	Estimate (RSE %)
k_{tr} (hour^{-1})	5.08 (8.7)
Effect of partial gastrectomy	1.46 (16.0)
Effect of total gastrectomy	3.14 (25.3)
CL_c/F_{CAP} (L/hour)	337 (5.3)
V_c/F_{CAP} (L)	207 (11.0)
Q_p/F_{CAP} (L/hour)	15.8 (8.2)
V_p/F_{CAP} (L)	31.4 (8.3)
CL_c/F_{dFCR} (L/hour)	148 (4.3)
V_c/F_{dFCR} (L)	20.5 (3.6)
Q_p/F_{dFCR} (L/hour)	94.1 (6.4)
V_p/F_{dFCR} (L)	39 (3.6)
$k_{dFUR>5\text{-}FU}$ (hour^{-1})	129 (2.9)
$k_{5\text{-}FU>FBAL}$ (hour^{-1})	777 (3.6)
Effect of *DPYD**2A heterozygous mutation	0.785 (11.2)
CL_c/F_{FBAL} (L/hour)	36.7 (5.2)
Effect of age	−0.97 (19.1)
Effect of gender female	0.757 (6.5)
V_c/F_{FBAL} (L)	84.7 (4.8)
Q_p/F_{FBAL} (L/hour)	11.7 (11.7)
V_p/F_{FBAL} (L)	39 (33.3)

BSV	%CV (RSE %), Shrinkage [%]
k_{tr} (hour^{-1})	60.7 (17.0) [38.6]
CL_c/F_{CAP} (L/hour)	57.5 (6.4) [6.6]
V_c/F_{CAP} (L)	132.1 (7.8) [12.6]
CL_c/F_{dFCR} (L/hour)	47.1 (4.4) [4.1]
$k_{dFUR>5\text{-}FU}$ (hour^{-1})	33.6 (6.0) [9.0]
$k_{5\text{-}FU>FBAL}$ (hour^{-1})	41.5 (6.0) [9.4]
CL_c/F_{FBAL} (L/hour)	32.3 (7.9) [15.6]
V_p/F_{FBAL} (L)	46.7 (4.7) [10.3]

BOV	%CV (RSE %), Shrinkage [%]
k_{tr} (hour^{-1})	57.4% (12.5) [44.6]

Correlations	Coefficient
ρ (BSV CL_c/F_{CAP}, V_c/F_{CAP})	0.53
ρ (BSV $k_{dFUR>5\text{-}FU}$, $k_{5\text{-}FU>FBAL}$)	0.63

Proportional RUV	%CV (RSE %), Shrinkage [%]
Capecitabine	57.6 (3.3) [4.3]
dFCR	40.5 (2.7) [6.1]
dFUR	42.7 (3.0) [6.3]
5-FU	37.7 (2.5) [3.9]
FBAL	30.4 (1.3) [7.7]

BSV, between-subject variability; BOV, between-occasion variability; RUV, residual unexplained variability; RSE, relative standard error; CV, coefficient of variation; k_{tr}, transit rate constant; CL_c/F, apparent clearance of central compartment; V_c/F, apparent central volume of distribution; Q_p/F, apparent intercompartmental clearance; V_p/F, apparent peripheral volume of distribution; k, rate constant; ρ, correlation coefficient; *DPYD*, dihydropyrimidine dehydrogenase; CAP, capecitabine; dFCR, 5'-deoxy-5-fluorocytidine; dFUR, 5'-deoxy-5-fluorouridine; 5-FU, 5-fluorouracil; FBAL, fluoro-β-alanine.

dFCR clearance from the central compartment (CL_c/F_{dFCR}), adequately described dFCR distribution and elimination.

Decay in the plasma concentrations of two metabolites, dFUR and 5-FU, illustrated great similarity to that of dFCR (**Figure S2**). Model runs in which the distribution volumes of dFUR and 5-FU were estimated ran into a boundary close to 0. These findings clearly indicated flip-flop PK for dFUR and 5-FU. Therefore, only the elimination rate constants for dFUR ($k_{dFUR>5\text{-}FU}$) and 5-FU ($k_{5\text{-}FU>FBAL}$) were estimated. BSV terms on these rate constants were successfully included. There was significant covariance between BSV in $k_{dFUR>5\text{-}FU}$ and $k_{5\text{-}FU>FBAL}$.

The decay in the plasma levels of the final metabolite FBAL occurred less rapidly than for capecitabine and the previous metabolites. Distribution and elimination of FBAL were best described with a two-compartment model. BSV on the apparent clearance (CL_c/F_{FBAL}) and distribution volume (V_c/F_{FBAL}) were successfully estimated.

Covariate model

An overview of the explored covariate–parameter associations is shown in **Table S1**. The estimated $k_{5\text{-}FU>FBAL}$ was 21.5% (relative standard error 11.2%) lower in patients who were heterozygous for the *DPYD**2A mutation (drop in objective function value (dOFV) −7.12). Patients carrying the *DPYD* c.1236G>A and c.2846A>T variants did not demonstrate altered 5-FU elimination. The estimated CL_c/F_{dFCR} was not affected by the heterozygous or homozygous *CDA* c.79A>C mutation. There was an effect of age (dOFV −40.71) and gender (dOFV −25.89) on CL_c/F_{FBAL}. Both the effect of age and gender were included in the final model. The effects of partial and total gastrectomy on the transit absorption rate were already incorporated in the first phase of model development.

Model evaluation

The fixed and random-effect parameters were estimated with adequate precision, as illustrated by relative standard errors of ≤ 33.3% and ≤ 17.0%, respectively (**Table 3**). Shrinkage was ≤ 15.6% for random-effect parameters accounting for BSV, although relatively high for random-effect parameters of BSV (38.6%) and BOV (44.6%) on k_{tr}. There was substantial unexplained variability on capecitabine plasma levels, as illustrated by the estimated proportional residual unexplained variability (RUV) of 57.6%. For the four metabolites, the proportional RUV was moderate with CV values ranging between 30.4–42.7%. Shrinkage on the proportional RUV parameters was low (≤7.7%). Overall, the population PK parameters were estimated with adequate precision. Goodness-of-fit plots for the final model (**Figure 2**) did not indicate model misspecification. The prediction-corrected visual predictive checks (pcVPC) demonstrated that capecitabine and metabolite PK were generally well described by the final PK model (**Figure 3**). Nevertheless, the median C_{max} levels for capecitabine and metabolites were slightly underpredicted. A three-compartmental distribution model for capecitabine was considered to improve the estimation of median C_{max} levels. This model
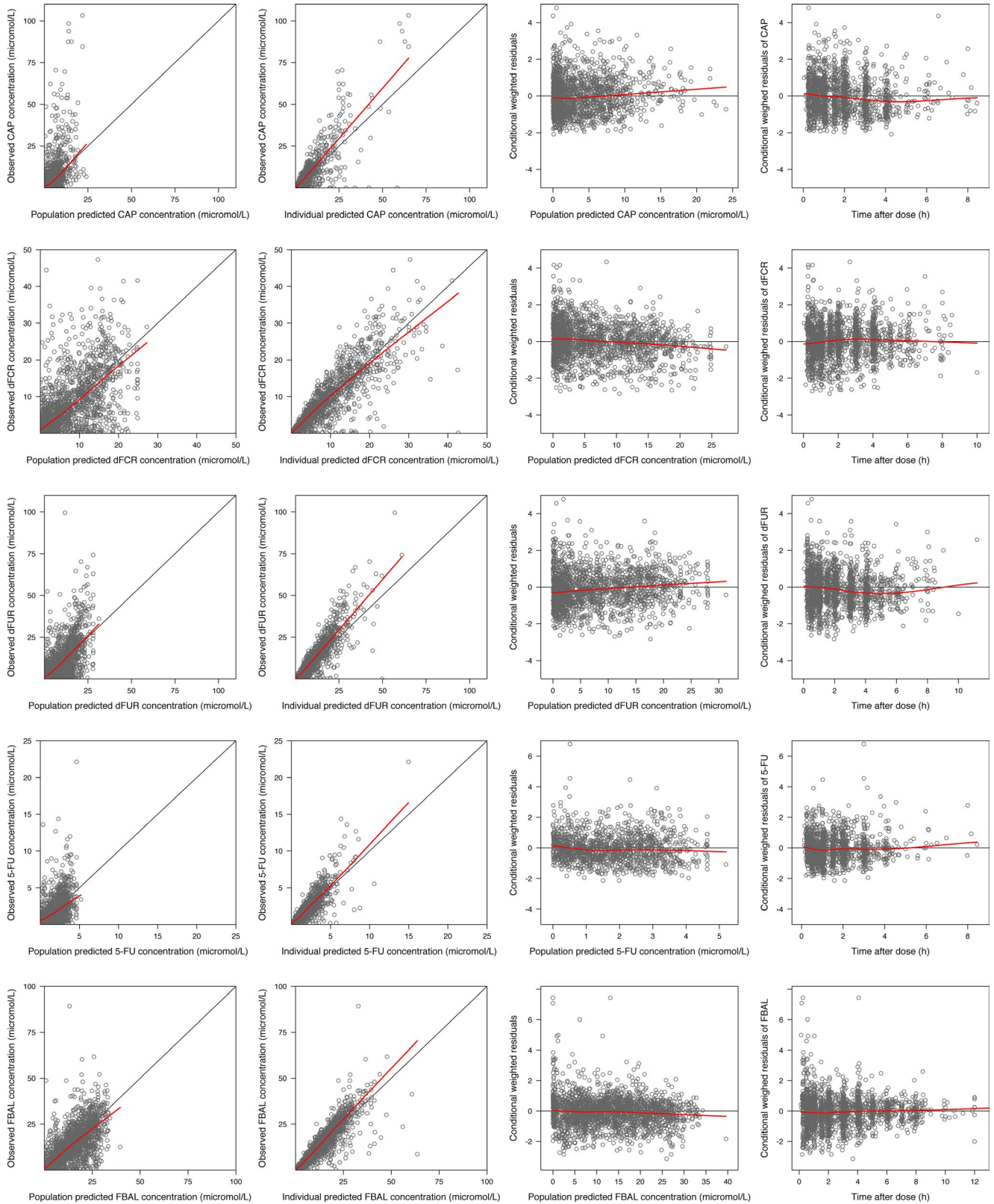
Figure 2 Goodness-of-fit plots for model-predicted capecitabine, dFCR, dFUR, 5-FU, and FBAL plasma concentrations. Black lines represent the lines of identity, and the red lines indicate the trend in observations. CAP, capecitabine; dFCR, 5′-deoxy-5-fluorocytidine; dFUR, 5′-deoxy-5-fluorouridine; 5-FU, 5-fluorouracil; FBAL, fluoro-β-alanine.
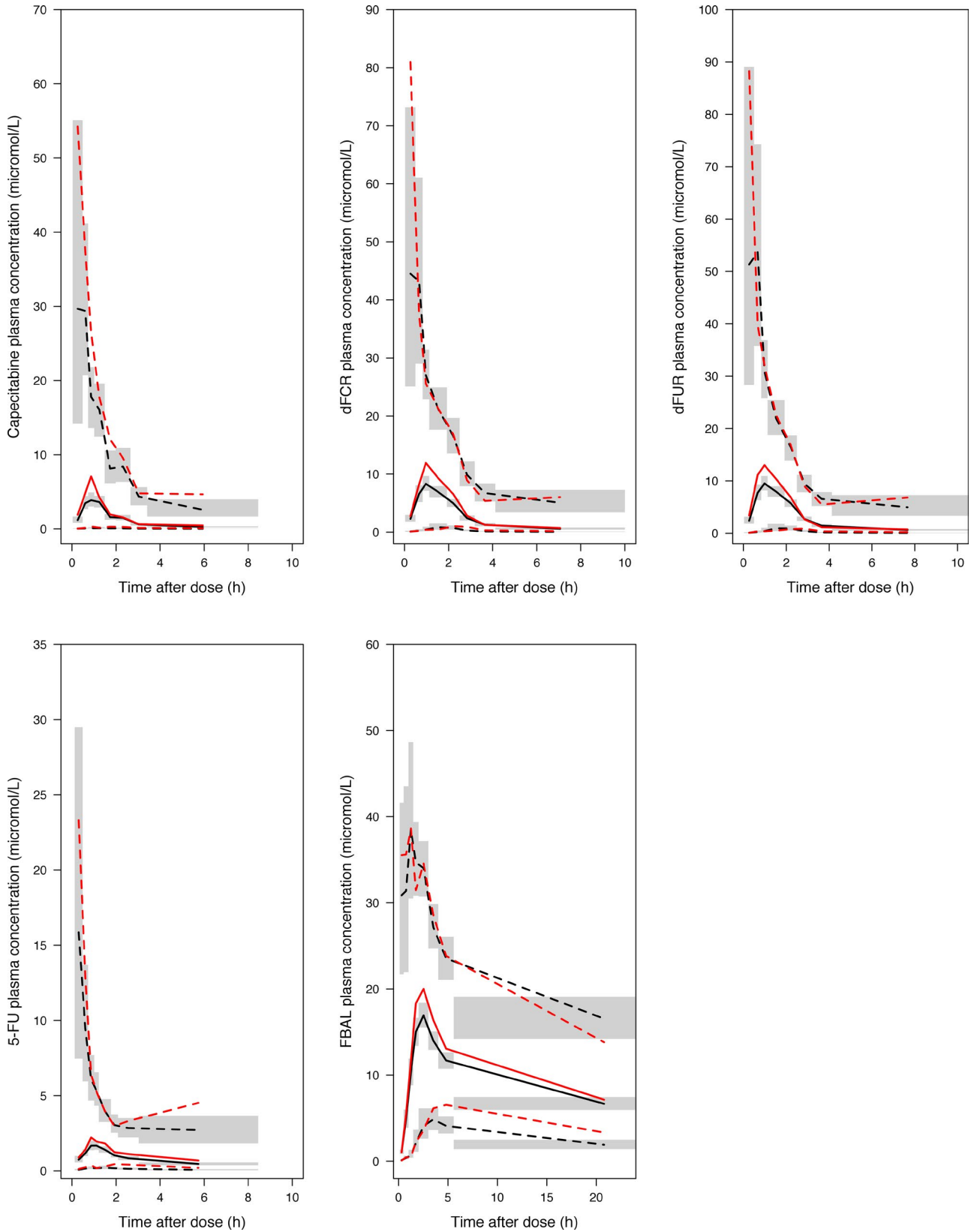
Figure 3 Prediction-corrected visual predictive checks of capecitabine, dFCR, dFUR, 5-FU, and FBAL. Red solid and black solid lines represent the median prediction-corrected observed and predicted data. Red dashed and black dashed lines illustrate the 5th and 95th percentiles of the prediction-corrected observed and predicted data. The gray shades illustrate the 95% confidence intervals of the simulated data. dFCR, 5′-deoxy-5-fluorocytidine; dFUR, 5′-deoxy-5-fluorouridine; 5-FU, 5-fluorouracil; FBAL, fluoro-β-alanine.

was, however, rejected because of poor parameter precision (overparameterization). Because capecitabine absorption is highly variable among and within subjects, it remained challenging to fully capture the complexity of this process within the PK model. Distribution of simulated transit absorption rates most probably deviated to some extent from the distribution in the observed transit absorption rates, which might have resulted in underprediction of the median C_{max} levels.

PK simulations

The effects of partial gastrectomy, total gastrectomy, and *DPYD**2A genomic mutation on the PK of capecitabine and metabolites were simulated. Simulation was, however, challenging because of the introduction of a zero-order absorption process during model building. As partial gastrectomy and total gastrectomy were found to be associated with faster transit rate absorption (higher k_{tr}), the introduction of a zero-order absorption model was assumed to be nonrandom and depending on gastrectomy status. Based on data records of first occasions, a zero-order absorption process was used during model building for 29%, 31.8%, and 50% of the curves from patients with nongastrectomy, partial gastrectomy, and total gastrectomy, respectively. These probabilities were used to randomly assign simulated patients to either zero-order absorption or transit rate absorption. In the case of zero-order absorption, the duration of the absorption was randomly resampled from the original data set with an upper boundary of 1 hour to avoid slow absorption (**Figure S3**). Complete absorption was expected during the assigned duration. Other PK parameters were simulated using the final PK model.

Simulated plasma concentration-time curves for capecitabine are shown in **Figure 4a**. The median capecitabine C_{max} (90% prediction interval (PI)) for the reference population (nongastrectomy) was 11.0 (2.7–39.9) mmol/L. After partial gastrectomy and total gastrectomy, the median capecitabine C_{max} (90% PI) were 13.0 (3.0–41.0) mmol/L and 16.7 (3.9–55.5) mmol/L, respectively. The median (90% PI) time to maximum capecitabine plasma levels (t_{max}) was 0.8 (0.3–3.3) hours for the reference population, 0.7 (0.3–2.4) hours after partial gastrectomy, and 0.4 (0.2–1.0) hours after total gastrectomy. Simulated PK profiles for dFCR and dFUR demonstrated similar results (**Figure S4a**). Peak levels of 5-FU were, besides gastrectomy status, also higher for patients carrying a *DPYD**2A mutation (**Figure 4b**; **Table S2**). Median 5-FU C_{max} values for patients with total gastrectomy and *DPYD**2A mutation were 70.7% in comparison to the reference population (nongastrectomy, *DPYD**2A wild type). FBAL concentration-time profiles were not affected by gastrectomy and *DPYD**2A status (**Figure S4b**).

DISCUSSION

We successfully developed a population PK model that adequately described the PK of capecitabine and its metabolites dFCR, dFUR, 5-FU, and FBAL in a large and heterogeneous population of cancer patients enriched for *DPYD**2A allele carriers and (partial) gastrectomy. This study is unique with respect to the number of included metabolites, variability among study populations, and

treatment schedules and with regard to the large total number of observations.

Capecitabine was rapidly absorbed, especially in patients who underwent partial or total gastrectomy. The physicochemical properties of the drug might be essential for this finding. Capecitabine is highly water soluble and shows good permeability.[14] Current data suggest that availability of gastric fluid is not required for the dissolution of capecitabine. The passage rate of capecitabine into the small bowel is increased after (partial) gastrectomy, which resulted in quick intestinal availability of capecitabine. Furthermore, this also implies adequate bioavailability of capecitabine and metabolites in cancer patients who have a history of bariatric surgery (i.e., Roux-en-Y gastric bypass).

Intake of food was previously found to delay capecitabine absorption.[14] Although capecitabine was preferably administered within 30 minutes after a meal in all seven studies, the amount and the type of food were not specified. It could be that the intake of food was reduced in patients who previously underwent gastrectomy, which in turn could have resulted in rapid capecitabine uptake. In general, the food effect could have been an important factor attributing to BOV and BSV in capecitabine absorption.

A first-pass effect seems to play a major role in the bioavailability of capecitabine and metabolites. The enzymes carboxylesterase, CDA, thymidine phosphorylase, and DPD are highly active in liver tissue.[15,16] Between-subject variability in enzymatic phenotypes, liver perfusion, and liver function likely contribute to variability in parameter estimates regarding capecitabine, dFCR, dFUR, and 5-FU PK.

The genetic polymorphism *CDA* c.79A>C, which has been associated with moderately decreased CDA activity,[17] did not show to significantly affect the CL_c/F_{dFCR}. Therefore, this genetic mutation might not be important for clinical practice.

Although the allele frequency of the *DPYD**2A allele in the general population is low (~1%),[9,13,18] data of a total of 21 variant allele carriers were available. For patients carrying the *DPYD**2A allele, the $k_{5-FU>FBAL}$ was estimated to be reduced by 21.5% (relative standard error 11.2%). Not all *DPYD**2A allele carriers, however, demonstrated a reduced DPD phenotype.[9] This could explain why the reduction in $k_{5-FU>FBAL}$ did not exceed 21.5% for patients carrying the *DPYD**2A allele. Previously, the *DPYD**2A allele has been associated with a 1.3-fold to 1.5-fold increase in 5-FU exposure after intravenous administration.[19]

Because *DPYD**2A allele carriers are at risk of severe early-onset fluoropyrimidine-induced toxicity, an initial dose reduction of 50% is recommended.[9,20] Nevertheless, the effect of the *DPYD**2A mutation on 5-FU elimination is less than expected, suggesting better treatment tolerability for this specific patient population. In case *DPYD**2A allele carriers do not experience clinically significant early capecitabine-induced toxicity after the initial dose reduction, it is recommended to increase the capecitabine dose during subsequent treatment cycles to prevent undertreatment.

Effects of the *DPYD* c.2846A>T and c.1236G>A variants on $k_{5-FU>FBAL}$ were explored, but were not statistically significant. Additional population PK analyses including larger numbers of *DPYD* c.2846A>T and c.1236G>A allele
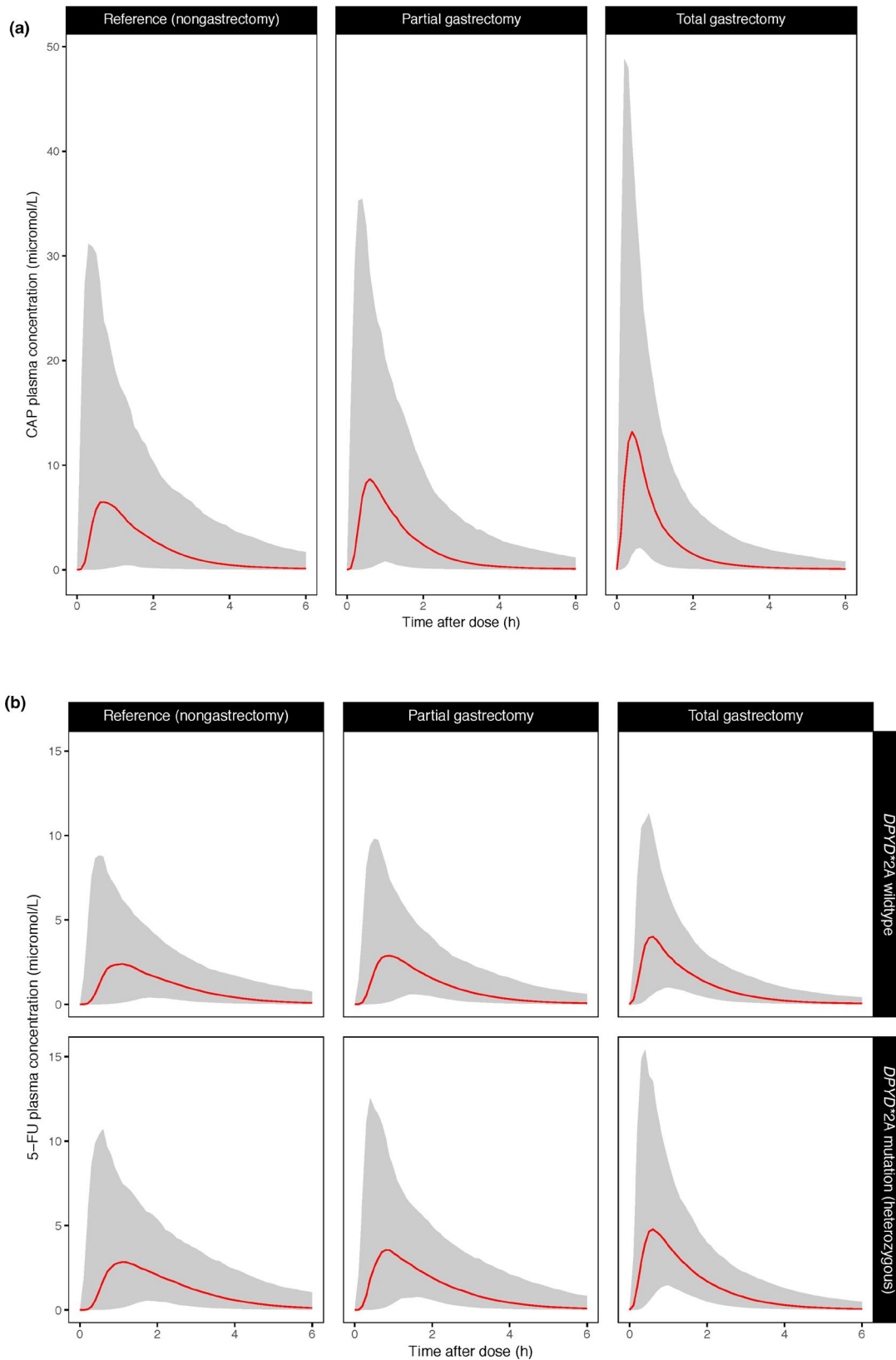
Figure 4 Simulations of capecitabine (**a**) and 5-FU (**b**) concentration-time profiles for patients with partial gastrectomy, total gastrectomy, and carriers of the *DPYD*2A genetic mutation after 2,000 mg of capecitabine. The red line represents the median predicted plasma concentrations. The gray shades illustrate the 90% prediction intervals. CAP, capecitabine; *DPYD*, dihydropyrimidine dehydrogenase; 5-FU, 5-fluorouracil.

carriers are warranted for improved analyses of possible covariate effects.

Two-compartmental distribution models were used for adequate description of capecitabine, dFCR, and FBAL distribution. None of the previously described population PK models by Gieschke *et al*. and Urien *et al*. included peripheral compartments.[6–8] Furthermore, we demonstrated that there is large BSV in the PK of capecitabine and dFCR. These two analytes were not included in the population PK models that were previously described by Gieschke *et al*.[6,7] By neglecting variability in capecitabine and dFCR PK, the previously developed models did not accurately reflect the source of variability in dFUR and 5-FU plasma exposure. Population PK studies described by Gieschke *et al*. mainly included the PK data of colorectal cancer patients who were treated with capecitabine monotherapy.[6,7] The currently described model was based on a more heterogeneous population of cancer patients who were treated with different capecitabine-based treatment regimens. This enabled us to identify the effect of gastrectomy on capecitabine absorption and the effect of the *DPYD**2A mutation on 5-FU elimination after capecitabine intake, which have not been described previously. The PK simulations demonstrated that capecitabine and 5-FU exposure is increased for *DPYD**2A carriers and after gastrectomy. Nonetheless, the prediction intervals of the simulation data showed overlap in 5-FU exposure among the different subpopulations. Therefore, it remains important to closely monitor each individual patient who is treated with capecitabine and apply dose modifications based on treatment tolerability.

In conclusion, a comprehensive population PK model of capecitabine and the metabolites dFCR, dFUR, 5-FU, and FBAL has been successfully developed and evaluated. This model adequately describes the complexity of capecitabine and metabolites PK in a large and heterogeneous population of cancer patients.

METHODS
Study population
Pooled data of seven clinical studies of capecitabine were used for the current analysis.[9,21–26] An overview of the studies is given in **Table 1**. In all studies, capecitabine was preferably administered within 30 minutes after food intake. Rich PK sampling designs were applied. Study 1 included patients who were heterozygous for the *DPYD**2A risk allele.[9] The other studies included patients with gastric, esophageal, colorectal, and anal cancer who were treated with capecitabine-based chemotherapy with or without radiotherapy. All studies were approved by the Medical Ethics Committee of The Netherlands Cancer Institute and were performed in compliance with the Declaration of Helsinki. Individual PK data were included for the current analysis if at least one observation for capecitabine, dFCR, dFUR, 5-FU, and FBAL was available, the individual *DPYD**2A status was known, and information on the time of sampling in relation to capecitabine administration was available. Actual times of capecitabine administration and sample collection were used for the population PK analysis.

Bioanalytical analysis and data handling
Capecitabine, dFCR, dFUR, 5-FU, and FBAL plasma concentrations were quantified using three validated liquid chromatography–tandem mass spectrometry (LC-MS/MS) assays.[27,28] Assay 1 was used for quantification of capecitabine, dFCR, and dFUR plasma concentrations in study 7 and for the first 27 patients who participated in study 3 (**Table 1**).[27] The remaining plasma concentrations of capecitabine, dFCR, and dFUR were quantified using assay 2.[28] The LLoQ for capecitabine, dFCR, and dFUR in assay 1 were 27.8, 40.8, and 40.6 nmol/L.[27] For assay 2, the LLoQ values were 139, 204, and 203 nmol/L.[28] Assay 1 and 2 were both validated in accordance with the US Food and Drug Admnistration guideline on bioanalytical method validation,[27,28] which assured comparable assay performance. The third LC-MS/MS assay was used to quantify all 5-FU and FBAL plasma concentrations.[28] The LLoQ for 5-FU and FBAL were 384 and 467 nmol/L.[28] Plasma concentrations below the LLoQ were not reported. For the absorption phase, the last observation below LLoQ that was obtained prior to the first observation above LLoQ was imputed in the data set as LLoQ/2. Including these observations as LLoQ/2 increased the amount of informative data that was needed for adequate modeling of the capecitabine absorption process.[29]

Population PK modeling
Nonlinear mixed-effects modeling using the software package NONMEM (version 7.3),[30] was applied for model development. Parameter estimation was achieved using the first-order conditional estimation method with interaction. R (version 3.3.0) was applied for data formatting and visualization.[31] Piraña (version 2.9.2) was used for model management.[32] The R package Xpose4 (version 4.5.3) and Perl-speaks NONMEM (PsN, version 4.4.8) were used for model diagnostics.[32]

Structural model development
Sequential population PK modeling was applied during the initial stage of model development. In the first step, a model of capecitabine PK was established. Estimated population PK parameters were then fixed and the base model was extended with the data of the first metabolite, dFCR. After optimization of the PK model for dFCR, the parameter estimates were fixed as well. The procedure of including PK data of the subsequent metabolite, model optimization, and fixing the population PK parameters was repeated until capecitabine and all four metabolites were included in the population PK model. After sequential optimization, all parameters were reestimated simultaneously using the structural model and parameter estimates of sequential analysis as initial values.

For capecitabine, several absorption models were examined during the first stage of model development: First-order absorption with lag time, combined zero-order and first-order absorption, mixture models of first-order absorption, and first-order transit absorption with a chain of transit compartments.[33] One-compartment and two-compartment models with first-order elimination were considered for the parent compound and the metabolites.

The phenomenon of flip-flop PK was evaluated by visual inspection. In the case of flip-flop PK, only the elimination rate

constant could be estimated for the specific metabolite. As the bioavailability of capecitabine and the fractions converted to the consecutive metabolites were structurally not identifiable, all parameters were estimated relative to these values.

Statistical model

BSV and BOV were estimated using an exponential model (Eq. 1):

$$\theta_{i,k} = \theta_{pop} \times \exp\left(\eta_i + \kappa_k\right) \qquad (1)$$

where $\theta_{i,k}$ represents the parameter estimate for individual i on occasion k, θ_{pop} the typical value for the population parameter, η_i being the individual-specific random effect from a normal distribution with mean zero and variance ω^2, and κ_k the occasion-specific random effect from a normal distribution with mean zero and variance π^2.

RUV was modeled using a combined additive and proportional model (Eq. 2):

$$C_{o,ij} = C_{p,ij} \times \left(1 + \varepsilon_{prop}\right) + \varepsilon_{add} \qquad (2)$$

where $C_{o,ij}$ represents the observed and $C_{p,ij}$ the model-predicted plasma concentration for individual i at timepoint j, and ε_{prop} and ε_{add} represent the proportional and additional residual error, respectively, which were assumed to be normally distributed with a mean of zero and variance σ^2. The variance of ε_{add} was fixed to the square of the LLoQ/2, taking the specific LLoQ for each assay into account.

Covariate model

Covariate–parameter associations were exclusively examined in case they were considered physiologically plausible. An overview of the explored covariates is given in **Table 2**. To accelerate the covariate analyses, fixed-effect and random-effect parameters upstream of the studied covariate–parameter associations were fixed.

The effect of age on model-predicted parameters was estimated as follows (Eq. 3):

$$\theta_i = \theta_{pop} \times \left(\frac{age_i}{age_{pop}}\right)^{\theta_{cov}} \qquad (3)$$

where age_i represents age of individual i, age_{pop} is the average age within the study population and θ_{cov} represents the covariate effect.

The effect of the categorical covariates gender, gastrectomy, and genetic polymorphisms were explored. Besides the effect of the *DPYD**2A mutation, the effect of the *DPYD* c.2846A>T and c.1236G>A mutations on 5-FU elimination were studied. The consequence of the *CDA* c.79A>C mutation on the apparent clearance of dFCR was also explored. Genetic polymorphisms were determined as described previously.[9,21,25,26]

The effect of the categorical covariates were modeled as follows (Eq. 4):

$$\theta_i = \theta_{pop} \times \theta_{cov}{}^{R_i} \qquad (4)$$

where R_i represents the covariate of interest with a value of 1 in presence of a specific covariate and with a value of 0 in absence of the covariate.

In case of missing categorical covariates a separate parameter for the missing group was estimated,[34] as follows (Eq. 5):

$$\theta_i = \theta_{pop} \times \theta_{missing} \qquad (5)$$

where $\theta_{missing}$ represents the covariate effect for the subjects with missing covariate data.

Model evaluation

Model evaluation was guided by goodness-of-fit plots,[35] pcVPC,[36] successful minimization, dOFV, and precision of obtained parameter estimates. Parameter precision was estimated using the COVARIANCE step in NONMEM. A drop in dOFV of > 3.84 with one degree of freedom, corresponding to a $P < 0.05$, was considered statistically significant for hierarchical models. The pcVPC of the final model was generated from 1,000 simulations. The 5th, 50th, and 95th percentiles of the prediction-corrected observations and simulations were visually compared. The combined error model allowed for simulation of negative plasma concentrations, which were replaced by LLoQ/2.

PK simulations

The final model was used to explore the effect of covariates on systemic exposure to capecitabine, 5-FU, and other metabolites. Therefore, concentration-time curves for capecitabine and metabolites were simulated ($n = 1,000$ individuals for each scenario) for a single capecitabine dose of 2,000 mg.

Supporting Information. Supplementary information accompanies this paper on the *CPT: Pharmacometrics & Systems Pharmacology* website (www.psp-journal.com).

Figure S1. Chemical structures and metabolic pathway of capecitabine, dFCR, dFUR, 5-FU, and FBAL. dFCR, 5′-deoxy-5-fluorocytidine; dFUR, 5′-deoxy-5-fluorouridine; 5-FU, 5-fluorouracil; FBAL, fluoro-β-alanine; CES, carboxylesterase; CDA, cytidine deaminase; TP, thymidine phosphorylase; DPD, dihydropyrimidine dehydrogenase; DHP, dihydropyriminidase; B-UP, β-ureidopropionase.
Figure S2. Log plasma concentration-time profiles of capecitabine, dFCR, dFUR, 5-FU, and FBAL. The red lines illustrate average plasma concentration-time profiles. CAP, capecitabine; dFCR, 5′-deoxy-5-fluorocytidine; dFUR, 5′-deoxy-5-fluorouridine; 5-FU, 5-fluorouracil; FBAL, fluoro-β-alanine.
Figure S3. Distribution of the durations of zero-order processes to describe rapid absorption during model building (first occasions only). The red dotted line illustrates the upper boundary that was applied during pharmacokinetic simulations.
Figure S4. Simulations of dFCR and dFUR (**a**) and FBAL (**b**) concentration-time profiles for patients with partial gastrectomy, total gastrectomy, and carriers of the *DPYD**2A genetic mutation after 2,000 mg of capecitabine. Simulated patients were of median age and female. The red lines represent the median predicted plasma concentrations. The gray shade illustrate the 90% prediction intervals. dFCR, 5′-deoxy-5-fluorocytidine; dFUR, 5′-deoxy-5-fluorouridine; FBAL, fluoro-β-alanine.
Table S1. Overview of evaluated covariate-parameter effects.
Table S2. Simulations of maximum plasma concentrations of 5-FU for patients with partial gastrectomy, total gastrectomy and carriers of the *DPYD**2A genetic mutation after 2,000 mg of capecitabine.

1. Judson, I.R. *et al.* A human capecitabine excretion balance and pharmacokinetic study after administration of a single oral dose of 14C-labelled drug. *Invest. New Drugs* **17**, 49–56 (1999).
2. Reigner, B., Blesch, K. & Weidekamm, E. Clinical pharmacokinetics of capecitabine. *Clin. Pharmacokinet.* **40**, 85–104 (2001).
3. Diasio, R.B. & Harris, B.E. Clinical pharmacology of 5-fluorouracil. *Clin. Pharmacokinet.* **16**, 215–237 (1989).
4. Longley, D.B., Harkin, D.P. & Johnston, P.G. 5-fluorouracil: mechanisms of action and clinical strategies. *Nat. Rev. Cancer* **3**, 330–338 (2003).
5. Heggie, G.D., Sommadossi, J.P., Cross, D.S., Huster, W.J. & Diasio, R.B. Clinical pharmacokinetics of 5-fluorouracil and its metabolites in plasma, urine, and bile. *Cancer Res.* **47**, 2203–2206 (1987).
6. Gieschke, R., Burger, H.-U., Reigner, B., Blesch, K.S. & Steimer, J.-L. Population pharmacokinetics and concentration-effect relationships of capecitabine metabolites in colorectal cancer patients. *Br. J. Clin. Pharmacol.* **55**, 252–263 (2003).
7. Gieschke, R., Reigner, B., Blesch, K.S. & Steimer, J.L. Population pharmacokinetic analysis of the major metabolites of capecitabine. *J. Pharmacokinet. Pharmacodyn.* **29**, 25–47 (2002).
8. Urien, S., Rezaí, K. & Lokiec, F. Pharmacokinetic modelling of 5-FU production from capecitabine–a population study in 40 adult patients with metastatic cancer. *J. Pharmacokinet. Pharmacodyn.* **32**, 817–833 (2005).
9. Deenen, M.J. *et al.* Upfront genotyping of DPYD*2A to individualize fluoropyrimidine therapy: a safety and cost analysis. *J. Clin. Oncol.* **34**, 227–234 (2016).
10. Meulendijks, D. *et al.* Clinical relevance of DPYD variants c.1679T>G, c.1236G>A/HapB3, and c.1601G>A as predictors of severe fluoropyrimidine-associated toxicity: a systematic review and meta-analysis of individual patient data. *Lancet. Oncol.* **16**, 1639–1650 (2015).
11. Jennings, B.A. *et al.* Evaluating predictive pharmacogenetic signatures of adverse events in colorectal cancer patients treated with fluoropyrimidines. *PLoS ONE* **8**, e78053 (2013).
12. Loganayagam, A. *et al.* Pharmacogenetic variants in the DPYD, TYMS, CDA and MTHFR genes are clinically significant predictors of fluoropyrimidine toxicity. *Br. J. Cancer* **108**, 2505–2515 (2013).
13. Lee, A.M. *et al.* DPYD variants as predictors of 5-fluorouracil toxicity in adjuvant colon cancer treatment (NCCTG N0147). *J. Natl. Cancer Inst.* **106**, 1–12 (2014).
14. Reigner, B. *et al.* Effect of food on the pharmacokinetics of capecitabine and its metabolites following oral administration in cancer patients. *Clin. Cancer Res.* **4**, 941–948 (1998).
15. Tabata, T. *et al.* Bioactivation of capecitabine in human liver: involvement of the cytosolic enzyme on 5'-deoxy-5-fluorocytidine formation. *Drug Metab. Dispos.* **32**, 762–767 (2004).
16. Naguib, F.N., el Kouni, M.H. & Cha, S. Enzymes of uracil catabolism in normal and neoplastic human tissues. *Cancer Res.* **45**, 5405–5412 (1985).
17. Gilbert, J.A. *et al.* Gemcitabine pharmacogenomics: cytidine deaminase and deoxycytidylate deaminase gene resequencing and functional genomics. *Clin. Cancer Res.* **12**, 1794–1803 (2006).
18. Rosmarin, D. *et al.* Genetic markers of toxicity from capecitabine and other fluorouracil-based regimens: Investigation in the QUASAR2 study, systematic review, and meta-analysis. *J. Clin. Oncol.* **32**, 1031–1039 (2014).
19. van Kuilenburg, A.B.P. *et al.* Evaluation of 5-fluorouracil pharmacokinetics in cancer patients with a c.1905+1G>A mutation in DPYD by means of a Bayesian limited sampling strategy. *Clin. Pharmacokinet.* **51**, 163–174 (2012).
20. Amstutz, U. *et al.* Clinical pharmacogenetics implementation consortium (CPIC) guideline for dihydropyrimidine dehydrogenase genotype and fluoropyrimidine dosing: 2017 update. *Clin. Pharmacol. Ther.* **103**, 210–216 (2018).
21. Deenen, M.J. *et al.* Phase 1a/1b and pharmacogenetic study of docetaxel, oxaliplatin and capecitabine in patients with advanced cancer of the stomach or the gastroesophageal junction. *Cancer Chemother. Pharmacol.* **76**, 1285–1295 (2015).
22. Jansen, E.P.M. *et al.* A phase I-II study of postoperative capecitabine-based chemoradiotherapy in gastric cancer. *Int. J. Radiat. Oncol. Biol. Phys.* **69**, 1424–1428 (2007).
23. Jansen, E.P.M. *et al.* Postoperative chemoradiotherapy in gastric cancer – a Phase I/II dose-finding study of radiotherapy with dose escalation of cisplatin and capecitabine chemotherapy. *Br. J. Cancer* **97**, 712–716 (2007).
24. Jansen, E.P.M., Boot, H., Dubbelman, R., Verheij, M. & Cats, A. Postoperative chemoradiotherapy in gastric cancer–a phase I-II study of radiotherapy with dose escalation of weekly cisplatin and daily capecitabine chemotherapy. *Ann. Oncol.* **21**, 530–534 (2010).
25. Joerger, M. *et al.* Germline TYMS genotype is highly predictive in patients with metastatic gastrointestinal malignancies receiving capecitabine-based chemotherapy. *Cancer Chemother. Pharmacol.* **75**, 763–772 (2015).
26. Deenen, M.J. *et al.* Simultaneous integrated boost-intensity modulated radiation therapy with concomitant capecitabine and mitomycin C for locally advanced anal carcinoma: a phase 1 study. *Int. J. Radiat. Oncol. Biol. Phys.* **85**, e201–e207 (2013).
27. Vainchtein, L.D., Rosing, H., Schellens, J.H.M. & Beijnen, J.H. A new, validated HPLC-MS/MS method for the simultaneous determination of the anti-cancer agent capecitabine and its metabolites: 5'-deoxy-5-fluorocytidine, 5'-deoxy-5-fluorouridine, 5-fluorouracil and 5-fluorodihydrouracil, in human plasma. *Biomed. Chromatogr.* **24**, 374–386 (2010).
28. Deenen, M.J., Rosing, H., Hillebrand, M.J., Schellens, J.H.M. & Beijnen, J.H. Quantitative determination of capecitabine and its six metabolites in human plasma using liquid chromatography coupled to electrospray tandem mass spectrometry. *J. Chromatogr. B. Analyt. Technol. Biomed. Life Sci.* **913-914**, 30–40 (2013).
29. Keizer, R.J. *et al.* Incorporation of concentration data below the limit of quantification in population pharmacokinetic analyses. *Pharmacol. Res. Perspect.* **3**, e00131 (2015).
30. Beal, S. & Sheiner, L. NONMEM User Guides (Icon Development Solutions, Ellicott City, MD, 1989).
31. R Development Core Team. R: A Language and Environment for Statistical Computing (R Foundation for Statistical Computing, Vienna, Austria, 2016).
32. Keizer, R.J., Karlsson, M.O. & Hooker, A. Modeling and simulation workbench for NONMEM: Tutorial on Pirana, PsN, and Xpose. *CPT pharmacometrics Syst. Pharmacol.* **2**, e50 (2013).
33. Rousseau, A. *et al.* Population pharmacokinetic modeling of oral cyclosporin using NONMEM: comparison of absorption pharmacokinetic models and design of a Bayesian estimator. *Ther. Drug Monit.* **26**, 23–30 (2004).
34. Keizer, R.J., Zandvliet, A.S., Beijnen, J.H., Schellens, J.H.M. & Huitema, A.D.R. Performance of methods for handling missing categorical covariate data in population pharmacokinetic analyses. *AAPS J.* **14**, 601–611 (2012).
35. Hooker, A.C., Staatz, C.E. & Karlsson, M.O. Conditional weighted residuals (CWRES): a model diagnostic for the FOCE method. *Pharm. Res.* **24**, 2187–2197 (2007).
36. Bergstrand, M., Hooker, A.C., Wallin, J.E. & Karlsson, M.O. Prediction-corrected visual predictive checks for diagnosing nonlinear mixed-effects models. *AAPS J.* **13**, 143–151 (2011).